A NIMA-related kinase, Cnk2p, regulates both flagellar length and cell size in *Chlamydomonas*

Brian A. Bradley and Lynne M. Quarmby*

Department of Molecular Biology and Biochemistry, Simon Fraser University, Burnaby, BC V5A 1S6, Canada

*Author for correspondence (e-mail: quarmby@sfu.ca)

Accepted 25 March 2005
Journal of Cell Science 118, 3317-3326 Published by The Company of Biologists 2005
doi:10.1242/jcs.02455

Summary

The cycle of ciliogenesis and ciliary disassembly is coordinated with cell division. In the unicellular alga *Chlamydomonas,* the two flagella are maintained at constant and equal length during interphase, and are reabsorbed prior to mitosis. We report that the NIMA-related kinase, Cnk2p, is an axonemal protein that affects flagellar length via effects on disassembly rate and also plays a role in the cellular assessment of size prior to committing to mitosis. This is the second NIMA-related kinase shown to affect ciliary function and cell cycle progression in *Chlamydomonas.* We speculate that members of the NIMA family have evolved nuanced roles to coordinate cilia/cell cycle regulation.

Key words: Axoneme, Cell cycle, Cilia, Nek

Introduction

Regulation of cell size requires the coordination of cell growth and cell division. *Saccharomyces cerevisiae* accomplishes this by enforcing a critical size threshold for division (Hartwell and Unger, 1977; Johnston et al., 1977). This serves to maintain a constant mean cell size in the population and ensures that cells have the necessary resources to complete genome duplication and mitosis. Cell size regulation in metazoans is dependent upon cell type and influenced by extracellular signals, although it is likely that metazoan cells possess a primordial cell size threshold that prevents division at small cell sizes (reviewed by Jorgensen and Tyers, 2004). Recent data from *Chlamydomonas* indicate a link between cilia and cell size regulation (Mahjoub et al., 2002; Mahjoub et al., 2004).

Cilia (also known as flagella) are assembled via a process called intraflagellar transport (IFT). IFT was discovered in *Chlamydomonas* (Kozminski et al., 1993) and involves the anterograde and retrograde movement of large protein complexes (IFT particles) to and from the distal tip of the flagella, driven by the microtubule-based motors kinesin-2 and cytoplasmic dynein, respectively (for reviews, see Rosenbaum and Witman, 2002; Cole, 2003). Flagellar components are constantly turning over at the distal tip: flagella are dynamic organelles (Marshall and Rosenbaum, 2001). Retrograde IFT is required for the recycling of IFT particles, but may not be required for flagellar disassembly (Pazour et al., 1998; Marshall and Rosenbaum, 2001; Parker and Quarmby, 2003).

A model for flagellar length control based on the steady-state balance of the kinetics of flagellar assembly and disassembly has emerged (Marshall and Rosenbaum, 2001; Marshall et al., 2005). Flagella assemble with length-dependent decelerating kinetics (Rosenbaum et al., 1969). The amount of IFT protein per flagellum is independent of length (Marshall and Rosenbaum, 2001; Marshall et al., 2005), suggesting that the length-dependence of assembly is due to increased travel time as the flagellum elongates (Marshall and Rosenbaum, 2001; Marshall et al., 2005). Flagellar disassembly, on the other hand, does not appear to be length-dependent (Marshall and Rosenbaum, 2001). The rapid resorption of flagella prior to mitosis occurs at a constant rate (Marshall et al., 2005). In addition, flagellar resorption rate is constant in temperature-sensitive *Chlamydomonas fla10-1* cells, where anterograde IFT is halted at the restrictive temperature (Kozminski et al., 1995; Marshall and Rosenbaum, 2001; Parker and Quarmby, 2003). These data have led to a kinetic model of length control in which flagella reach a steady-state length unique to the balance between the length-dependent rate of assembly and the constant rate of disassembly (Marshall and Rosenbaum, 2001; Marshall et al., 2005). Although kinetic regulation of length appears to play a central role in determining flagellar length, genetic data suggest that there may be additional mechanisms affecting length (reviewed by Marshall, 2004).

Three groups of *Chlamydomonas* mutants have aberrant flagellar length: *lf* (long flagella), *ulf* (unequal length flagella) and *shf* (short flagella) (McVittie, 1972; Jarvik et al., 1984; Barsel et al., 1988; Asleson et al., 1998). None of the *SHF* genes have been cloned and we know little about them. Two *ulf* mutants, *ulf1* and *ulf3,* are null alleles of the *LF3* gene (Tam et al., 2003). Point mutations in *LF3*, like mutations in *LF1, LF2,* and *LF4* cause long flagella. The gene products of *LF1, LF2* and *LF3* do not localize to flagella and instead they may form a complex in the cell body (Tam et al., 2003; Nguyen et al., 2005). Intriguingly, *LF4* encodes a flagellar protein related to mammalian MOK, a MAP kinase of unknown function (Berman et al., 2003). Wilson and Lefebvre (Wilson and Lefebvre, 2004) showed that another kinase, *Chlamydomonas* GSK3, partially localizes to flagella and contributes to flagellar length control.

We now report that *Chlamydomonas* NIMA-related kinase 2 (Cnk2p) influences both flagellar length and cell size. The

first NIMA-related kinase discovered in *Chlamydomonas* was Fa2p (Mahjoub et al., 2002). *fa2* mutants are slow to transit the cell cycle owing to a G2-M delay and do not sever the nine outer doublet microtubules of the axoneme in response to deflagellation stimuli (Finst et al., 1998; Mahjoub et al., 2002). During interphase, Fa2p localizes to the proximal end of the flagella, whereas during mitosis it is associated with the polar region of the mitotic spindle (Mahjoub et al., 2004). This was the first report of a NIMA-related kinase with both cell cycle and ciliary functions; Cnk2p is the second.

NIMA-related kinases are defined by sequence similarity to the kinase domain of the *Aspergillus* protein, NIMA (never in mitosis A), which is essential for mitotic progression (Osmani et al., 1991). Eukaryotes that lack cilia, such as fungi and higher plants, only have one or a few members of this family (Osmani et al., 1991; Kambouris et al., 1993; Krien et al., 1998). Organisms with ciliated cells, such as *Chlamydomonas* and humans, have ten or eleven members (reviewed by O'Connell et al., 2003; Bradley et al., 2004) (our unpublished observations). This, in conjunction with the association Fa2p with cilia, raises the possibility that this gene family has cilia-related functions in addition to established cell cycle roles (reviewed by O'Connell et al., 2003).

We have manipulated levels of Cnk2p in order to study its role in *Chlamydomonas*. Expression of HA epitope-tagged Cnk2p produces small cells with short flagella, whereas knockdown of endogenous CNK2 via RNAi produces large cells with long flagella. Analyses of parameters that affect cell size and flagellar length indicate that Cnk2p regulates flagellar length by promoting flagellar disassembly and regulates cell size by affecting the assessment of cell size prior to mitosis (commitment size).

Materials and Methods

Cell strains, culture and genetic crosses

Chlamydomonas reinhardtii strains *fla10-1* (CC-1919), *pf3* (CC-1026), *pf9* (CC-1254), *pf14* (CC-1032), *pf18* (CC-1036), *oda9* (CC-2244) *and mat3-4* (CC-3994) were provided by the *Chlamydomonas* Genetics Center (Duke University, Durham, NC). Wild-type strain B214 was provided by G. Pazour (University of Massachusetts, Worcester, MA). The *fa2-1* mutant was isolated in our lab (Finst et al., 1998). Genetic crosses were performed using standard techniques to obtain the strains *fla10*:CNK2-HA, *fla10*:CNK2-RNAi, *pf3*:CNK2-HA, *pf9*:CNK2-HA, *pf14*:CNK2-HA, *pf18*:CNK2-HA and *oda9*:CNK2-HA (Harris, 1989). Cnk2p-HA and CNK2-RNAi strains were backcrossed into a B214 background prior to subsequent experiments. All cells were maintained on TAP (Tris-Acetate-Phosphate) media plates (Harris, 1989) supplemented with 1.5% agar, under constant illumination at 20°C.

Expression constructs and nuclear transformation

The pCNK2-HA expression construct (Fig. 1A) is derived from pGenD kindly provided by J. Rochaix, University of Geneva, Geneva, Switzerland (Fischer and Rochaix, 2001). The *ble* coding sequence (start codon to stop codon) was removed from pGenD by digestion with *Nde*I and *Eco*RI (New England Biolabs, Beverly, MA; Invitrogen, Burlington, ON) to be replaced by the *CNK2* coding sequence. The *CNK2* coding sequence was amplified with *Pfu* Turbo polymerase (Stratagene, La Jolla, CA) from the cloned cDNA (Bradley et al., 2004) using primers designed to include *Nde*I and *Eco*RI restriction sites at the start and just before the stop codons, respectively (forward, 5′-CGATCATATGGCGAAGGACGGGTCT-AAGG-3′ and reverse, 5′-CGATGAATTCCCACCCGCGCGCTGG-CCGCGG-3′). The product was digested with *Nde*I and *Eco*RI, and ligated using T4 DNA ligase (Invitrogen) to the pGenD backbone. The 3XHA epitope tag (kindly provided by S. Dutcher, Washington University, St Louis, MO) was amplified with *Taq* polymerase (Qiagen, Mississauga, ON) using primers that incorporated *Eco*RI restriction sites and a stop codon (forward, 5′-CTGAGAAT-TCTACCCCTACGACGTGCCCGAC-3′ and reverse, 5′-TGATATC-GAATTCCTAGCCCGGGGGCCGGCG-3′). The product was digested with *Eco*RI and ligated into the unique *Eco*RI site at the 3′ end of the *CNK2* coding sequence (Fig. 1A). The selectable marker *ble,* providing resistance to Zeocin (Invitrogen) driven by the rubisco promoter and UTRs, was excised from pSP124S (kindly provided by S. Purton, University College London, London, UK) (Lumbreras et al., 1998) using flanking *Hin*dIII restriction sites and ligated to pCNK2-HA at a unique *Hin*dIII site downstream of the PsaD 3′ UTR (Fig. 1A).

Construction of pCNK2-RNAi (Fig. 3A) was initiated by excising the epitope-tagged CNK2 coding sequence from pCNK2-HA by digestion with *Nde*I and *Eco*RI. Primers designed to include *Nde*I and *Eco*RI sites (forward, 5′-CGATCATATGTGGAAGAACCGGCCC-TACTCG-3′ and reverse, 5′-ATCGGAATTCCTGCCACGGCGAGG-GCTGTTG-3′) were used to amplify 977 bp (basepairs 546-1523, numbering from the start codon) of the *CNK2* cDNA with *Taq* polymerase. The product was digested and ligated to the pCNK2-HA backbone. The resulting plasmid was digested with *Bsi*WI (New England Biolabs) and *Eco*RI. Primers designed to include *Eco*RI sites (forward, 5′-CGATGAATTCTGGAAGAACCGGCCCTACTCG-3′ and reverse, 5′-ATCGGAATTCCTGCCACGGCGAGGGCTGTTG-3′) were used to amplify the same 977 bp of the CNK2 cDNA with *Taq* polymerase. The product was digested with *Bsi*WI and *Eco*RI and ligated to the above *Bsi*WI/*Eco*RI-digested plasmid to generate pCNK2-RNAi (Fig. 3A).

All primers were synthesized by Invitrogen and final constructs were verified by sequencing (Center for Molecular Medicine and Therapeutics, Vancouver, BC). All constructs were linearized by *Vsp*I (Promega, Madison, WI) digestion prior to transformation of *Chlamydomonas*. Nuclear transformations were performed as previously described (Finst et al., 1998), except that cultures were diluted with 10 ml TAP media after vortexing with glass beads, and incubated overnight in constant light with agitation. After pelleting, cultures were plated on TAP plates containing 30 μg/ml Zeocin.

Cell fractionation and immunoblot analysis

Cell bodies, flagella, axonemes and membrane plus matrix fractions were isolated as previously described (Witman, 1986). Immunoblot analysis of cellular fractions was performed as previously described (Mahjoub et al., 2004). Cell equivalents of each fraction were separated by SDS-PAGE (10%) and blotted to supported nitrocellulose (BioRad, Mississauga, ON). Blots were probed with rat monoclonal anti-HA (1:1000; clone 3f10; Roche Diagnostics, Basel, SUI), washed and then probed with horseradish peroxidase (HRP)-conjugated goat anti-rat IgG (1:2500; Amersham Biosciences, Baie d'Urfe, QC). Blots were stripped and reprobed with mouse monoclonal anti-α-tubulin (1:10,000; clone B-5-1-2; Sigma Aldrich). After washing, the blot was probed with HRP-conjugated horse anti-mouse IgG (1:10,000; Vector Laboratories, Burlingame, CA). The ECL chemiluminescent detection system (Amersham Biosciences) was used for visualization.

Indirect immunofluorescence imaging

Indirect immunofluorescence was conducted as described (Mahjoub et al., 2004), using a DeltaVision imaging station (Applied Precision, Issaquah, WA). Primary antibodies used in this study are as follows:

rat monoclonal anti-HA (1:200; clone 3f10; Roche Diagnostics), mouse monoclonal anti-centrin (1:400; clone 20h5; kindly provided by J. Salisbury, Mayo Clinic, Rochester, MN), and mouse monoclonal anti-α-tubulin (1:500; clone B-5-1-2; Sigma Aldrich). Secondary antibodies used are as follows: Texas Red-conjugated goat anti-rat IgG (1:200; for Cnk2p-HA), Alexa 350-conjugated goat anti-mouse $IgG2_b$ (1:200; for centrin) and Alexa 488-conjugated goat anti-mouse IgG1 (1:200; for α-tubulin). All secondary antibodies were obtained from Molecular Probes (Eugene, OR).

Flagellar length and cell size measurements

Flagellar length, cell width and cell length were measured by DIC microscopy using the measurement tools provided with the Softworx (v. 3.22) software package. Cell volumes were calculated based on the ellipsoid shape of *Chlamydomonas* cells using the formula $4/3\pi[L/2][W/2]^2$ (Umen and Goodenough, 2001), where L is cell length and W is cell width. Only flagellated cells were measured for volume estimates.

Protein content per cell was calculated from cells harvested growing in TAP media under continuous light. Cell density was determined using a hemacytometer, following autolysin treatment of all three cultures to release cells from mother cell walls. 1×10^6 cells were pelleted, resuspended in 50 μl of 0.5× SDS sample buffer and boiled for 5 minutes. 5 μl lysate was used to determine protein concentration using the Advanced Protein Assay Reagent (Cytoskeleton, Denver, CO) with BSA (BioRad) as a standard. Cell counts and protein determinations were done blind and in triplicate for all three cultures.

Cell synchrony experiments

For mitotic index experiments, cultures were grown in minimal media at 22°C with bubbling (5% CO_2) for 3 days on a 14 hour light/10 hour dark regime. On the fourth day, cultures were left in the light and were sampled over the next 24 hours. Mitotic index was determined by microscopic examination for the presence of cleavage furrows; in *Chlamydomonas*, incipient cleavage furrows form at preprophase and are visible throughout mitosis and cytokinesis (Kirk, 1998).

To determine the number of times each cell divided, we used cultures that were grown in TAP media for several days in constant light. Aliquots of the culture were plated on minimal media and placed in the dark for 24 hours (Umen and Goodenough, 2001). The plates were then examined using a dissecting microscope and scored for the number of cells per microcolony. The number of cells observed was used to calculate the number of division cycles the founder cell underwent. To determine commitment size and growth rate, cultures were grown in minimal media for several days in constant light and shifted to the dark for 24 hours (Umen and Goodenough, 2001). Samples were taken immediately after the shift to light (for commitment size determination) and every 2 hours thereafter (for growth rate determination).

Flagellar regeneration and resorption experiments

For flagellar regeneration experiments, 5 ml of each overnight culture grown in TAP media was transferred into 15 ml centrifuge tubes. A 100 μl sample, defined as the pre-deflagellation time point, was fixed in 2% glutaraldehyde. To induce deflagellation, 5 ml of 40 mM sodium acetate, 1 mM $CaCl_2$, pH 4.5, with or without 10 μg/ml cycloheximide was added to the cultures, which were mixed by inversion. Cells were pelleted by centrifugation at 1000 ***g*** for 1 minute and resuspended in 5 ml TAP media with or without 10 μg/ml cycloheximide. A 100 μl sample, defined as the zero time point, was fixed, and the cultures were placed at 22°C in constant light with shaking. 100 μl samples were fixed every 15 minutes thereafter. For flagellar disassembly experiments, 2-day-old cultures on TAP plates were flooded with 10 mM HEPES-KOH (pH 7.2) and the cultures were left unagitated for 2 hours at 22°C to obtain flagellated cells. Cells were pipetted into 15 ml centrifuge tubes and pelleted by centrifugation at 1000 ***g*** for 3 minutes. Then the cells were resuspended in 10 mM HEPES-KOH (pH 7.2) prewarmed to 33°C. A 100 μl sample, defined as the zero time-point, was fixed and the cultures were placed in a 33°C incubator with constant light. 100 μl samples were taken every hour. All samples were fixed in 2% glutaraldehyde.

Northern analysis

Northern analysis was performed as described previously (Mahjoub et al., 2002) with the following modifications: ~0.5 kb probes for CNK2 (basepairs 107-767 of the cDNA) and β-tubulin (basepairs 963-1546 of the genomic sequence) were generated using [α-^{32}P]dCTP (3000 Ci/mmol) with the Prime-it II random primer labeling kit (Stratagene). Probes were purified using a PCR purification kit (Qiagen) and hybridized to blots at 10^6 cpm/ml at 70°C overnight and washed as described (Virca et al., 1990); blots were visualized using a Storm phosphoimager (Molecular Dynamics, Sunnyvale, CA). Before reprobing, blots were stripped by washing three times in 0.1 M NaOH for 30 seconds.

Results

Cnk2p localizes to puncta along the length of the axoneme

To determine the localization of Cnk2p we generated an HA epitope-tagged expression construct (Fig. 1A). This construct makes use of the promoter and UTRs from the intronless *Chlamydomonas* PsaD gene to drive constitutive expression of cDNA-derived coding sequences (Fischer and Rochaix, 2001). We also inserted the selectable marker gene *ble* (Lumbreras et al., 1998), to allow selection of transformants on Zeocin plates following nuclear transformation. Two independent transformants expressing Cnk2p-HA were isolated, backcrossed and characterized (see below; Table 1).

Subcellular fractionation of cells expressing Cnk2p-HA revealed that Cnk2p-HA is targeted to the flagella (Fig. 1B). The small amount of Cnk2p-HA detected in the cell body fraction may either be due to flagellar contamination or Cnk2p-HA associated with basal bodies (see below). Detergent

Table 1. Flagellar length and cell volume measurements for various strains of *Chlamydomonas reinhardtii* grown in TAP (rich) media

Strain	Mean flagellar length (μm)	Mean cell volume (μm^3)	*n*
B214 (WT parental)	10.1±0.27	175±12.2	500
Cnk2p-HA #70*	7.8±0.14	118±7.3	500
Cnk2p-HA #210	7.9±0.30	115±10.2	200
CNK2-RNAi #7	10.7±0.45	230±11.7	200
CNK2-RNAi #8	11.2±0.37	259±17.1	200
CNK2-RNAi #13	11.1±0.42	219±12.4	200
CNK2-RNAi #20*	12.4±0.21	302±15.8	500
CNK2-RNAi #22	11.2±0.36	246±8.9	200
fa2-1	10.2±0.26	306±13.4	200
mat3-4	10.2±0.19	104±8.4	200
shf1	7.3±0.26	171±10.2	200
lf3-2	17.2±1.80	179±13.7	200

Reported values are the mean±s.e.m. Values are derived from at least two independent experiments with at least 100 measurements per experiment.

*Cnk2p-HA and CNK2-RNAi strains which were used for genetic crosses and experiments reported in this manuscript.

extraction of the flagellar fraction reveals that Cnk2p-HA is a component of the axoneme and is not associated with the membrane plus matrix fraction (Fig. 1B). This result is consistent with data from the flagellar proteome project, which found endogenous Cnk2p in the axonemal fraction (Greg Pazour and George Witman, University of Massachusetts, Worcester, MA, personal communication).

To refine the localization of Cnk2p-HA we performed indirect immunofluorescence using anti-HA antibodies (Fig. 1C). We triple-stained wild-type cells and those expressing Cnk2p-HA with anti-α-tubulin to reveal the flagella and cortical array of microtubules (Doonan and Grief, 1987), anti-centrin to label the distal striated fibers connecting the basal bodies at the base of the flagella, as well as the nucleus-basal body connectors (Salisbury et al., 1988; Sanders and Salisbury, 1989), and anti-HA to localize Cnk2p-HA. The Cnk2p-HA signal is observed in puncta along the length of the flagella as well as at the basal bodies (Fig. 1C). Two examples of Cnk2p-HA expressing cells are shown, one with basal body staining (middle panels) and another that lacks basal body staining (right-hand panels in Fig. 1C).

To determine which structures within the axoneme Cnk2p-HA might be associated with, genetic crosses were performed with Cnk2p-HA cells and various flagellar mutants. Indirect immunofluorescence was used to determine whether Cnk2p-HA was mislocalized in mutants lacking the dynein regulatory complex (*pf3*), inner dynein arms (*pf9*), radial spokes (*pf14*), central pair microtubules (*pf18*) or outer dynein arms (*oda9*) (reviewed by Porter and Sale, 2000). Cnk2p-HA localization was undisturbed in all of these mutant backgrounds (Fig. 2) suggesting that Cnk2p-HA is associated with the outer doublet microtubules.

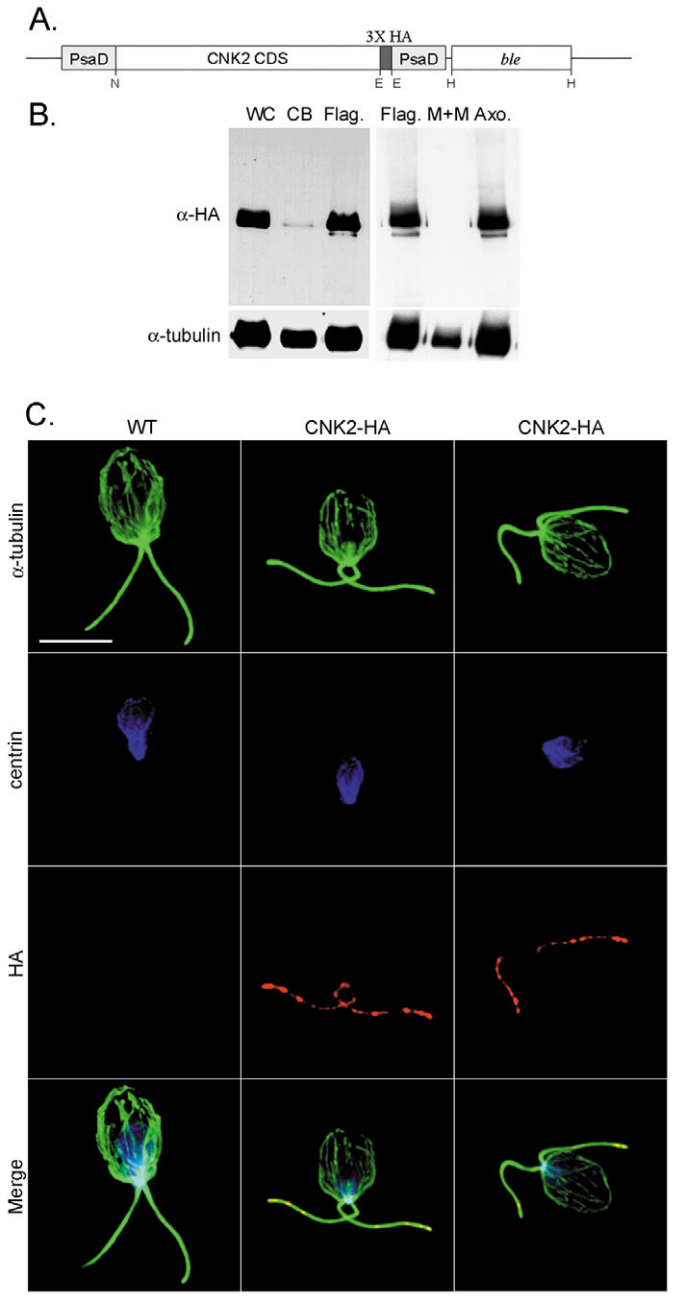

Aberrant levels of CNK2 expression affect cell size and flagellar length

A CNK2-RNAi expression construct (Fig. 3A) was designed to express an inverted repeat of the CNK2 coding sequence that is predicted to generate a dsRNA hairpin upon transcription. Northern analysis of stable nuclear transformants showed a reduction in *CNK2* mRNA levels as low as 15% of wild-type levels (strain 20), when normalized to β-tubulin mRNA levels (Fig. 3B,C). CNK2-RNAi strain 20 was used in subsequent experiments.

We observed that Cnk2p-HA cells have short flagella and CNK2-RNAi cells have long flagella (Table 1; Fig. 4A). We also noticed cell size effects: Cnk2p-HA cells are smaller than wild-type cells and CNK2-RNAi cells are larger than the wild type (Table 1; Fig. 4B). The altered cell volumes reflect a change in biomass: in one experiment done in triplicate, total protein/cell was 27.7±0.6 pg/cell (wild type), 18.0±0.2 pg/cell (Cnk2p-HA) and 34.8±1.3 pg/cell (CNK2-RNAi). In order to test whether flagellar length is a consequence of cell size we examined a number of mutant strains (Table 1). Mutant *fa2-1* cells, which are similar in size to the CNK2-RNAi cells, have flagella of wild-type length; *mat3-4* cells, which are similar in size to the Cnk2p-HA cells (when both are grown in TAP media) have wild-type length flagella; conversely, flagellar length mutants, *shf1* and *lf3-2*, have normal cell sizes (Table 1). We conclude that flagellar length phenotypes are not a trivial consequence of changes in cell size.

Fig. 1. Cnk2p-HA is an axonemal protein. (A) Schematic representation of the CNK2-HA expression construct, containing the *CNK2* coding sequence (CDS) with the 3XHA epitope tag on the C-terminus. The PsaD promoter and UTRs are used to drive constitutive expression (Fischer and Rochaix, 2001). E, *Eco*RI; H, *Hin*dIII; N, *Nde*I restriction sites. (B) Immunoblot analysis of cell fractions from Cnk2p-HA expressing cells probed with an anti-HA antibody. Blots were stripped and reprobed with an anti-α-tubulin antibody. Cell equivalent amounts of whole cells (WC), cell bodies (CB) and flagella (Flag) were loaded in each lane (left-hand blot). Stoichiometric amounts of flagella (Flag), membrane and matrix fraction (M+M), and axonemal fractions (Axo) were loaded in each lane (right-hand blot). (C) Wild type and two examples of Cnk2p-HA cells triple-stained for indirect immunofluorescence with anti-α-tubulin, anti-HA and anti-centrin antibodies. Bar, 5 μm.

Effects of Cnk2p levels on flagellar assembly and disassembly

To determine how Cnk2p affects flagellar length, we examined several parameters that influence the steady-state length of flagella. Specifically, we tested rates of flagellar assembly and disassembly, as well as the size of the axonemal precursor pool within the cell body.

To examine the net flagellar assembly rate we measured flagellar regeneration post-deflagellation (Fig. 5A, closed symbols). Wild-type, Cnk2p-HA and CNK2-RNAi cultures were induced to deflagellate by a brief pH shock. All strains were observed to regenerate flagella with similar kinetics, but the CNK2-RNAi cells initiated regeneration sooner (compare 15 minute time-points) and the Cnk2p-HA flagella stopped growing at a shorter length.

When deflagellated in the presence of 10 μg/ml cycloheximide, protein synthesis is halted, yet cells regenerate short flagella, indicating the presence of a cytoplasmic pool of flagellar precursors (Rosenbaum et al., 1969). In order to assess whether the precursor pools were of similar size in our strains we repeated the flagellar regeneration time course in the presence of 10 μg/ml cycloheximide (Fig. 5A, open symbols). Both the Cnk2p-HA and the CNK2-RNAi strains were capable of regenerating flagella similar in length to those of the wild-type strain, suggesting that precursor pool size is similar to that in the wild type in our strains.

To assess relative rates of flagellar disassembly, Cnk2p-HA and CNK2-RNAi strains were crossed into a *fla10-1* mutant background; *fla10-1* is a temperature-sensitive mutant carrying a point mutation in a subunit of the heterotrimeric kinesin-2 anterograde IFT motor (Walther et al., 1994). At the permissive temperature (20°C) *fla10-1* cells have wild-type length flagella,

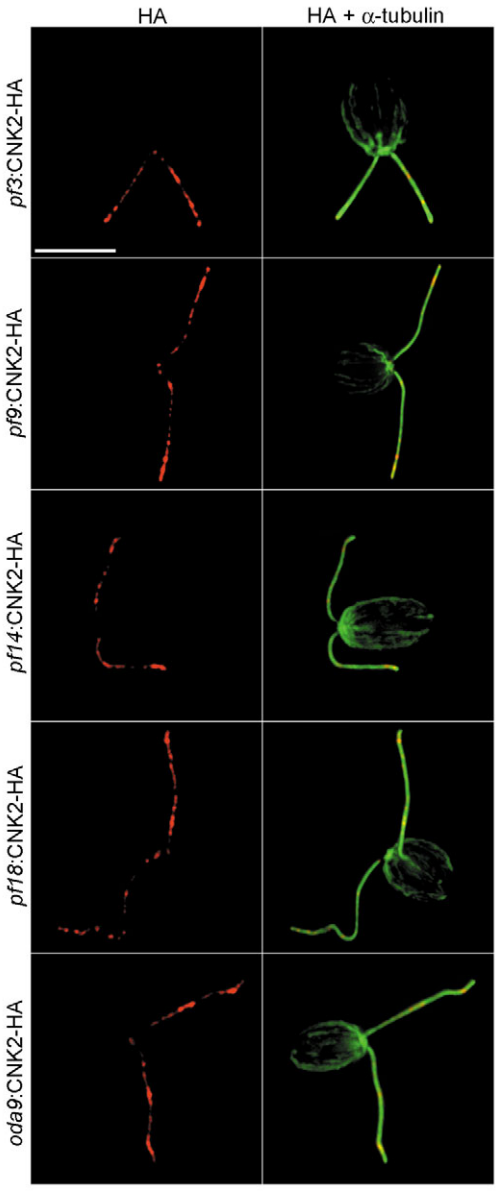

Fig. 2. Cnk2p-HA is not associated with established axonemal accessory structures. Indirect immunofluorescence of cells expressing Cnk2p-HA in axoneme structural mutant backgrounds using anti-HA and anti-α-tubulin. *pf3*, lacks dynein regulatory complex; *pf9*,lacks inner dynein arms; *pf14*, lacks radial spokes; *pf18*, lacks central pair; *oda9*, lacks outer dynein arms. Bar, 5 μm.

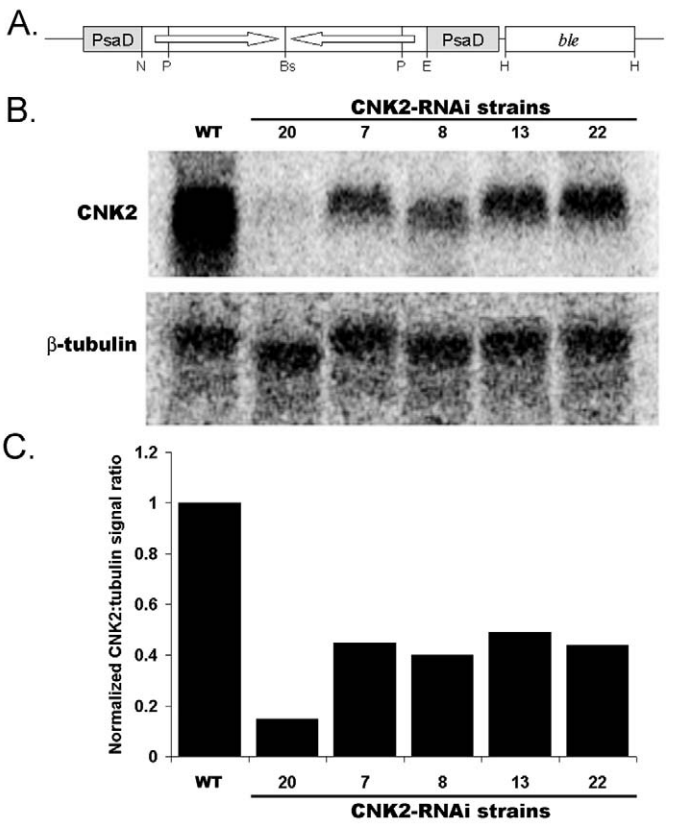

Fig. 3. Knockdown of CNK2 expression via RNAi. (A) Schematic representation of the CNK2-RNAi expression construct. The construct, designed to generate 834 bp of dsRNA upon expression, was used to produce stable RNAi strains by nuclear transformation. Bs, *Bsi*WI ; E, *Eco*RI; H, *Hin*dIII; N, *Nde*I; P, *Pst*I restriction sites. (B) Northern analysis of CNK2 transcript levels in five independent CNK2-RNAi transformants. 15 μg total RNA was loaded in each lane. The blot was probed with 0.5 kb of ^{32}P labeled CNK2 cDNA, stripped and reprobed with 0.5 kb of ^{32}P labeled β-tubulin cDNA. (C) The ratio of CNK2 message to tubulin message was determined by comparing band intensities using ImageQuant v2.0. CNK2-RNAi strain 20 was used in all subsequent experiments.

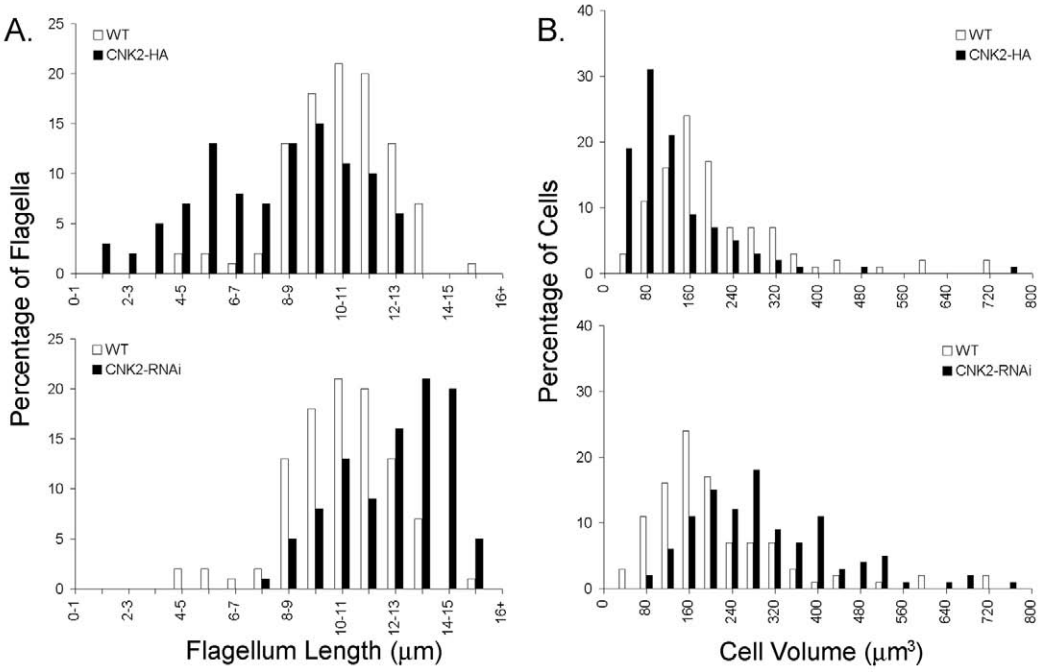

Fig. 4. Aberrant Cnk2p levels affect cell size and flagellar length distributions. (A) Flagellar length distributions for the wild type (WT), Cnk2p-HA and CNK2-RNAi. (B) Cell volume distributions for wild type, Cnk2p-HA and CNK2-RNAi. For each strain, 100 cells or flagella (one per cell) were measured in three independent experiments and pooled to generate the distributions.

but at the restrictive temperature (33°C), in the absence of added calcium, cells resorb their flagella, presumably owing to continued disassembly in the absence of anterograde IFT (Adams et al., 1982; Marshall and Rosenbaum, 2001; Parker and Quarmby, 2003). To determine whether Cnk2p levels affect resorption rate, *fla10-1* cells and cells expressing Cnk2p-HA or CNK2-RNAi in a *fla10-1* background, were allowed to assemble flagella at the permissive temperature and were then shifted to the restrictive temperature (Fig. 5B). We observed that *fla10-1* and *fla10-1*:CNK2-RNAi cells resorb flagella at the

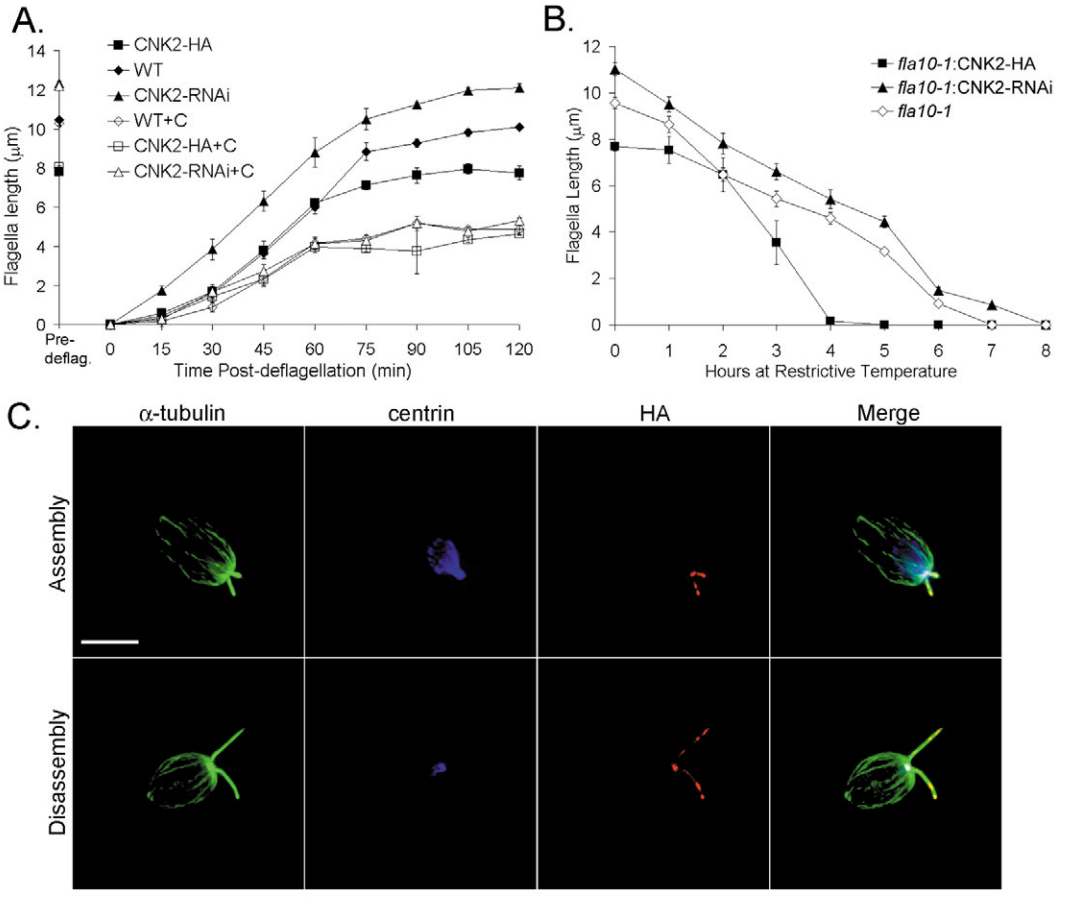

Fig. 5. Analysis of flagellar dynamics in Cnk2p-HA and RNAi strains. (A) Flagellar lengths were measured during recovery from pH shock in the presence or absence of 10 μg/ml cycloheximide. 40 flagella were measured for each time-point for each of three independent experiments, error bars represent s.e.m. (B) Flagellar lengths during resorption of flagella in *fla10-1*:Cnk2p-HA and *fla10-1*:CNK2-RNAi strains after shift to restrictive temperature. 40 flagella were measured for each time-point for each of three independent experiments, error bars represent s.e.m. (C) Cnk2p-HA cells assembling flagella post deflagellation and disassembling flagella prior to mitosis, triple-stained for indirect immunofluorescence with anti-α-tubulin, anti-HA and anti-centrin. Bar, 5 μm.

same overall rate (~1.4 μm/hour), whereas the *fla10-1*:Cnk2p-HA expressing cells resorb their flagella more quickly (Fig. 5B). Importantly, the *fla10-1*:Cnk2p-HA cells displayed a lag period followed by rapid resorption; the rate of resorption, once it gets started, is more than twice as fast as the other strains (3.4 μm/hour).

We also examined the localization of Cnk2p-HA during flagellar assembly and resorption (Fig. 5C). During both flagellar assembly post-deflagellation (Fig. 5C, upper row) and flagellar disassembly prior to mitosis (Fig. 5C, lower row), Cnk2p-HA accumulates at the basal bodies, but is also present in puncta along the flagella. We were unable to detect Cnk2p-HA during mitosis by indirect immunofluorescence of synchronized cultures (data not shown).

Effects of Cnk2p levels on cell cycle parameters

We previously reported that another *Chlamydomonas* mutant, *fa2*, has large cells due at least in part to a G2-M delay (Mahjoub et al., 2002). To determine whether the cell size phenotypes of Cnk2p-HA and CNK2-RNAi are also due to effects on cell cycle progression, we looked at the timing of mitotic entry by examining synchronized cultures for the presence of cleavage furrows. The smaller Cnk2p-HA cells enter mitosis sooner than the wild type whereas the larger CNK2-RNAi cells enter mitosis later than the wild type and slightly ahead of *fa2-1* cells (Fig. 6A). In order to determine whether the cell cycle progression and mean cell size differences were due to effects on growth rate, we assessed the growth of wild-type, Cnk2p-HA and CNK2-RNAi strains. Cells of all three strains grow at similar rates (Fig. 6B).

In *Chlamydomonas,* cells undergo a prolonged G1 phase during which they grow until they reach a threshold size when cells commit to at least one round of division (Pickett-Heaps, 1975). Subsequently, the cells undergo multiple rounds of rapidly alternating S and M phases, producing 2, 4, 8 or 16 daughter cells of equal size (Coleman, 1982; Craigie and Cavalier-Smith, 1982; Donnan and John, 1983). The number of divisions is determined by cell size at commitment. Very little is known about the regulation of commitment size in *Chlamydomonas,* except that cells with mutations in a retinoblastoma protein (RB) homologue, Mat3p, are small due to a decrease in commitment size and an increase in the number of rounds of division post commitment (Umen and Goodenough, 2001).

To test whether the number of rounds of division post commitment was altered in Cnk2p-HA and CNK2-RNAi strains, we grew cultures in rich (TAP) media for several days in constant light and plated the cultures on minimal media in the dark for 24 hours. Under these conditions the cells have no

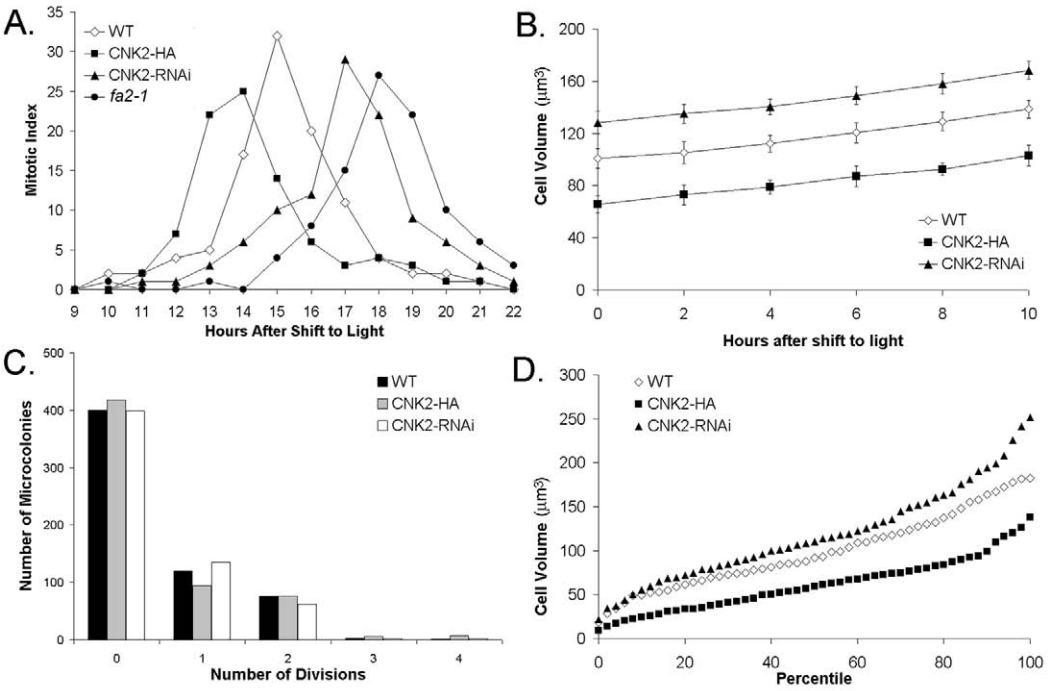

Fig. 6. Aberrant Cnk2p levels affect cell cycle progression. (A) Mitotic index measurements of wild-type (WT), CNK2-HA, CNK2-RNAi and *fa2-1* cultures. Cultures were synchronized by alternating light-dark cycles for 3 days and examined microscopically on day 4 for the percentage of cells with cleavage furrows. A total of 200 cells were examined for each time-point, from two independent experiments (100/experiment). (B) Growth of WT, CNK2-HA and CNK2-RNAi cells. Cultures were grown in minimal media for several days in constant light and placed in the dark for 24 hours. Cultures were shifted back to the light to initiate growth and samples were taken every 2 hours. A total of 200 cells were measured for each time-point from two independent experiments (100/experiment), error bars represent s.e.m. (C) Analysis of the number of division cycles post commitment. Cultures were grown in TAP media for several days, plated on minimal media, and placed in the dark for 24 hours. Colonies were examined microscopically to determine the number of cells per colony. A total of 600 colonies were scored from two independent experiments (300/experiment). (D) Commitment size measurement. Cultures were grown as in B, and a sample was fixed immediately after the shift to light. A total of 300 cells were measured from each culture in three independent experiments (100/experiment).

energy source and thus stop growing, but any cells larger than the commitment size are expected to divide, and the divisions observed will be from one round of rapid S and M phase cycling. We did not observe a change in the number of rounds of division post commitment (Fig. 6C). Because we do not observe a change in growth rate or in the number of divisions post-commitment, we hypothesized that a change in the commitment threshold would generate both the cell size and mitotic entry phenotypes that we see in our strains.

To test this hypothesis we held cultures in minimal media in the dark for 24 hours, during which time cells larger than the commitment size are expected to divide (Umen and Goodenough, 2001). Thus, the largest cells in the population after 24 hours in the dark should be at or near the commitment size threshold. From this experiment, we estimate the commitment size for the wild type to be 182 μm^3, which is similar to previously reported values (Fig. 6D) (Umen and Goodenough, 2001; Mahjoub et al., 2002). Importantly, the commitment size for Cnk2p-HA and CNK2-RNAi was different from the wild type: the Cnk2p-HA strain had a commitment threshold of 137 μm^3 whereas the CNK2-RNAi strain committed to divide at or above 257 μm^3 (Fig. 6D). These commitment size estimates can be used to predict the fraction of cells in a culture that will divide when plated on minimal media and kept in the dark. In one experiment we used our commitment size estimates to predict that 33% of the wild-type, Cnk2p-HA and Cnk2p-RNAi cells would go on to divide on minimal media in the dark. We observed 37%, 28% and 33% of cells divided at least once during the 24 hour dark period for wild-type, Cnk2p-HA and Cnk2p-RNAi cells respectively, thus confirming that the effects of Cnk2p expression on commitment size is at least as large as estimated. We conclude that Cnk2p levels affect commitment size.

Discussion

We have shown that the NIMA-related kinase, Cnk2p is an axonemal protein both by subcellular fractionation (Fig. 1B), and by immunofluorescent localization of Cnk2p-HA (Fig. 1C). Genetic analyses using axonemal mutants indicate that Cnk2p is not associated with known accessory axonemal structures, suggesting an intimate association with the outer doublet microtubules (Fig. 2). This is the third report of a member of this cell cycle-associated family of kinases in cilia (Mahjoub et al., 2004; Wloga et al., 2003).

Cnk2p appears to play a role in flagellar length control. Expression of Cnk2p-HA produces short flagella comparable in length to those of *shf1* mutants (Table 1). Conversely, knockdown of Cnk2p expression produces flagella longer than the wild type, but not as long as *lf* mutants, which can have flagella three to four times the wild-type length (Table 1) (Barsel et al., 1988). Our data indicate that when protein synthesis is inhibited during flagellar regeneration, wild-type, Cnk2p-HA and CNK2-RNAi cells grow flagella of similar length (Fig. 5A). This is not surprising as all three strains have similar levels of Cnk2p post deflagellation, i.e. very little, because virtually all of the Cnk2p is shed with the flagella. It does however suggest that the axonemal precursor pool is the same size in all three strains, indicating that the length phenotypes are not due to a change in the availability of precursors. We found that the rate of flagellar assembly following deflagellation was similar to the wild type in both HA and RNAi strains (Fig. 5A). However, it is important to note that CNK2-RNAi cells initiate assembly sooner. This may reflect regulation of a gating mechanism/check point at the base of the flagellum that controls access of IFT particles and flagellar precursors to the elongating flagellum (Kirk, 1989; Rosenbaum and Witman, 2002; Beech, 2003) or a change in the rate of recovery from the pH shock (Quarmby, 1996). We found that *fla10-1*:CNK2-RNAi cells disassemble flagella at the same rate as *fla10-1* cells, but expression of Cnk2p-HA caused more rapid loss of flagella (Fig. 5B). Thus an increase in the amount of Cnk2p caused increased rates of disassembly, while retaining net assembly rates similar to the wild type, until the flagella approached their steady-state length (Fig. 5A). We propose that disassembly is inhibited during the initial stages of flagellar assembly as previously proposed (Parker and Quarmby, 2003) and suggest a model wherein Cnk2p is active during the initiation of flagellar assembly and at steady state.

Chlamydomonas cells undergo rapid flagellar resorption prior to mitosis. Owing to the effects of Cnk2p on both flagellar resorption and cell cycle progression, Cnk2p might serve to promote pre-mitotic flagellar resorption. One possibility is that Cnk2p functions as part of a *Chlamydomonas* RB pathway. Mutants in *mat3*, which are defective in *Chlamydomonas* RB, have a smaller commitment threshold than the wild type (Umen and Goodenough, 2001), and although vegetative *mat3* cells have flagella of wild-type length (Table 1), *mat3* gametes have short flagella (Armbrust et al., 1995). A dominant allele of *MAT3* and extragenic suppressors of *mat3-4* have been isolated and shown to cause a large cell phenotype (Umen et al., 2003), it will be of interest to determine whether these cells also have flagella of comparable length to CNK2-RNAi cells.

In order to determine how Cnk2p might regulate cell size, we studied the effects of expression level on various cell cycle parameters. Expression of Cnk2p-HA produces small cells, whereas knockdown of CNK2 expression produces large cells (Fig. 4B; Table 1). These cell size defects are due to alterations in the mitotic commitment size threshold (Fig. 6D). Cnk2p-HA cells enter mitosis sooner than the wild type (Fig. 6A) because, with wild-type rates of cell growth (Fig. 6B), they pass the smaller commitment size threshold sooner. Because the number of rounds of division following commitment is similar to the wild type (Fig. 6C), the resulting daughter cells are small, and again because growth rate is similar to the wild type, the cell size distribution of the population is shifted towards small cells (Fig. 4B). The same logic explains the size phenotype of CNK2-RNAi cells.

Another axonemal protein might also regulate commitment size: phototropin, a blue-light receptor in *Chlamydomonas,* has been localized to the axoneme and, like Cnk2p-HA, this localization is not disturbed in mutants lacking accessory axonemal structures (Huang et al., 2004). Blue light treatment increases the size threshold for commitment (Oldenhof et al., 2004). Although it is not known whether phototropin is the receptor responsible for the effect on commitment size, the presence of a C-terminal serine/threonine kinase domain in phototropin suggests that this receptor may be part of a signaling pathway that alters commitment. It will be interesting to determine whether Cnk2p and phototropin are participating in the same pathway.

Cnk2p is the second NIMA-related kinase found to be

axonemal. Fa2p has recently been reported to localize to the proximal end of the axoneme in *Chlamydomonas* at a site known as the SOFA (site of flagellar autotomy) (Mahjoub et al., 2004), a site to which these authors also find that exogenously expressed Fa2p-EGFP in ciliated mouse kidney cells localizes. The conservation of Fa2p localization suggests that one or more mammalian NIMA-related kinases may be axonemal. We have previously noted that expansion of the NIMA-related family of proteins correlates with the presence of ciliated cells in the lineage (Bradley et al., 2004). Of the ten known NIMA-related kinase genes in *Chlamydomonas*, only two have been studied to date (FA2 and CNK2) and both affect ciliary disassembly and the cell cycle. Further correlation of cilia with NIMA-related kinases derives from the association of Neks with ciliopathies. Mutations in murine Nek1 or Nek8 produce cystic kidneys similar to those found in patients with polycystic kidney diseases (Upadhya et al., 2000; Liu et al., 2002). The genesis of kidney cysts is not completely understood, but there is a convergence of diverse data indicating that defective signaling from the primary cilia is the proximal cause of aberrant cell proliferation leading to cystic kidneys (reviewed by Pazour, 2004). We speculate that members of the NIMA-related kinase family play important roles in the coordinated regulation of cilia and the cell cycle in other organisms or cell types with cilia.

We are grateful to Jeff Salisbury, Susan Dutcher, Saul Purton, Peter Hegemann and J. P. Rochaix, for centrin antibodies, 3XHA epitope-tag, pSP124S, pSI103 and pGenD, respectively. Nick Inglis, Bari Zahedi, and especially Jeremy Parker and Moe Mahjoub are thanked for their varied and valuable contributions. We are particularly indebted to Jim Umen whose critical reading of an earlier draft of this manuscript led to significant improvement in some of the experiments. The thoughtful comments of two anonymous reviewers are also appreciated. This work was funded by operating grants to L.M.Q. from NSERC (RGPIN 227132) and CIHR (MOP 37861). B.A.B. is supported by graduate fellowships from NSERC and MSFHR.

References

Adams, G. W., Huang, B. and Luck, D. J. (1982). Temperature-sensitive assembly-defective flagella mutants of *Chlamydomonas reinhardtii*. *Genetics* **100**, 579-586.

Armbrust, E. V., Ibrahim, A. and Goodenough, U. W. (1995). A mating type-linked mutation that disrupts the uniparental inheritance of chloroplast DNA also disrupts cell-size control in *Chlamydomonas*. *Mol. Biol. Cell* **6**, 1807-1818.

Asleson, C. M. and Lefebvre, P. A. (1998). Genetic analysis of flagellar length control in *Chlamydomonas reinhardtii*: a new long-flagella locus and extragenic suppressor mutations. *Genetics* **148**, 693-702.

Barsel, S. E., Wexler, D. E. and Lefebvre, P. A. (1988). Genetic analysis of long-flagella mutants of *Chlamydomonas reinhardtii*. *Genetics* **118**, 637-648.

Beech, P. L. (2003). The long and the short of flagellar length control. *J. Phycol.* **39**, 837-839.

Berman, S. A., Wilson, N. F., Haas, N. A. and Lefebvre, P. A. (2003). A novel MAP kinase regulates flagellar length in *Chlamydomonas*. *Curr. Biol.* **13**, 1145-1149.

Bradley, B. A., Wagner, J. J. and Quarmby, L. M. (2004). Identification and sequence analysis of six new members of the NIMA-related kinase family in *Chlamydomonas*. *J. Eukaryot. Microbiol.* **51**, 66-72.

Cole, D. G. (2003). The intraflagellar transport machinery of *Chlamydomonas reinhardtii*. *Traffic* **4**, 435-442.

Coleman, A. W. (1982). The nuclear cell cycle in *Chlamydomonas* (Chlorophyceae). *J. Phycol.* **18**, 192-195.

Craigie, R. A. and Cavalier-Smith, T. (1982). Cell volume and the control of the *Chlamydomonas* cell cycle. *J. Cell Sci.* **54**, 173-191.

Donnan, L. and John, P. C. (1983). Cell cycle control by timer and sizer in *Chlamydomonas*. *Nature* **304**, 630-633.

Doonan, J. H. and Grief, C. (1987). Microtubule cycle in *Chlamydomonas reinhardtii*: an immunofluorescence study. *Cell Motil. Cytoskel.* **7**, 381-392.

Finst, R. J., Kim, P. J. and Quarmby, L. M. (1998). Genetics of the deflagellation pathway in *Chlamydomonas*. *Genetics* **149**, 927-936.

Fischer, N. and Rochaix, J. D. (2001). The flanking regions of PsaD drive efficient gene expression in the nucleus of the green alga *Chlamydomonas reinhardtii*. *Mol. Genet. Genomics* **265**, 888-894.

Harris, E. H. (1989). The *Chlamydomonas* sourcebook: a comprehensive guide to biology and laboratory use. San Diego: Academic Press.

Hartwell, L. H. and Unger, M. W. (1977). Unequal division in *Saccharomyces cerevisiae* and its implications for the control of cell division. *J. Cell Biol.* **75**, 422-435.

Huang, K., Kunkel, T. and Beck, C. F. (2004). Localization of the bluelight receptor phototropin to the flagella of the green alga *Chlamydomonas reinhardtii*. *Mol. Biol. Cell* **15**, 3605-3614.

Jarvik, J. W., Reinhart, F. D., Kuchka, M. R. and Adler, S. A. (1984). Altered flagellar size-control in *shf-1* short flagella mutants of *Chlamydomonas reinhardtii*. *J. Protozool.* **31**, 199-204.

Johnston, G. C., Pringle, J. R. and Hartwell, L. H. (1977). Coordination of growth with cell division in the yeast *Saccharomyces cerevisiae*. *Exp. Cell Res.* **105**, 79-98.

Jorgensen, P. and Tyers, M. (2004). How cells coordinate growth and division. *Curr. Biol.* **14**, R1014-R1027.

Kambouris, N. G., Burke, D. J. and Creutz, C. E. (1993). Cloning and genetic analysis of the gene encoding a new protein kinase in *Saccharomyces cerevisiae*. *Yeast* **9**, 141-150.

Kirk, D. L. (1998). *Volvox*. New York: Cambridge University Press.

Kozminski, K. G., Johnson, K. A., Forscher, P. and Rosenbaum, J. L. (1993). A motility in the eukaryotic flagellum unrelated to flagellar beating. *Proc. Natl. Acad. Sci. USA* **90**, 5519-5523.

Kozminski, K. G., Beech, P. L. and Rosenbaum, J. L. (1995). The *Chlamydomonas* kinesin-like protein FLA10 is involved in motility associated with the flagellar membrane. *J. Cell Biol.* **131**, 1517-1527.

Krien, M. J., Bugg, S. J., Palatsides, M., Asouline, G., Morimyo, M. and O'Connell, M. J. (1998). A NIMA homologue promotes chromatin condensation in fission yeast. *J. Cell Sci.* **111**, 967-976.

Liu, S., Lu, W., Obara, T., Kuida, S., Lehoczky, J., Dewar, K., Drummond, I. A. and Beier, D. R. (2002). A defect in a novel Nek-family kinase causes cystic kidney disease in the mouse and in zebrafish. *Development* **129**, 5839-5846.

Lumbreras, V., Stevens, D. R. and Purton, S. (1998). Efficient foreign gene expression in *Chlamydomonas reinhardtii* mediated by an endogenous intron. *Plant J.* **14**, 441-448.

Mahjoub, M. R., Montpetit, B., Zhao, L., Finst, R. J., Goh, B., Kim, A. C. and Quarmby, L. M. (2002). The FA2 gene of *Chlamydomonas* encodes a NIMA family kinase with roles in cell cycle progression and microtubule severing during deflagellation. *J. Cell. Sci.* **115**, 1759-1768.

Mahjoub, M. R., Rasi, M. Q. and Quarmby, L. M. (2004). A NIMA-related Kinase, Fa2p, localizes to a novel site in the Proximal cilia of *Chlamydomonas* and mouse kidney cells. *Mol. Biol. Cell* **15**, 5172-5186.

Marshall, W. F. (2004). Cellular length control systems. *Annu. Rev. Cell Dev. Biol.* **20**, 677-693.

Marshall, W. F. and Rosenbaum, J. L. (2001). Intraflagellar transport balances continuous turnover of outer doublet microtubules: implications for flagellar length control. *J. Cell Biol.* **155**, 405-414.

Marshall, W. F., Qin, H., Brenni, M. R. and Rosenbaum, J. L. (2005). Flagellar length control system: testing a simple model based on intraflagellar transport and turnover. *Mol. Biol. Cell* **16**, 270-278.

McVittie, A. (1972). Flagellum mutants of *Chlamydomonas reinhardtii*. *J. Gen. Microbiol.* **71**, 525-540.

Nguyen, R. L., Tam, L. W. and Lefebvre, P. A. (2005). The LF1 gene of *Chlamydomonas reinhardtii* encodes a novel protein required for flagellar length control. *Genetics* **169**, 1415-1424.

O'Connell, M. J., Krien, M. J. and Hunter, T. (2003). Never say never. The NIMA-related protein kinases in mitotic control. *Trends Cell Biol.* **13**, 221-228.

Oldenhof, H., Bisova, K., van den Ende, H. and Zachleder, V. (2004). Effect of red and blue light on the timing of cyclin-dependent kinase activity and the timing of cell division in *Chlamydomonas reinhardtii*. *Plant Physiol. Biochem.* **42**, 341-348.

Osmani, A. H., McGuire, S. L. and Osmani, S. A. (1991). Parallel activation of the NIMA and p34/cdc2 cell cycle-regulated protein kinases is required to initiate mitosis in *A. nidulans*. *Cell* **67**, 283-291.

Parker, J. D. and Quarmby, L. M. (2003). *Chlamydomonas fla* mutants reveal a link between deflagellation and intraflagellar transport. *BMC Cell Biol.* **4**, 11.

Pazour, G. J. (2004). Intraflagellar transport and cilia-dependent renal disease: the ciliary hypothesis of polycystic kidney disease. *J. Am. Soc. Nephrol.* **15**, 2528-2536.

Pazour, G. J., Wilkerson, C. G. and Witman, G. B. (1998). A dynein light chain is essential for the retrograde particle movement of intraflagellar transport (IFT). *J. Cell Biol.* **141**, 979-992.

Pickett-Heaps, J. D. (1975). *Green Algae*. Sunderland: Sinauer Associates.

Porter, M. E. and Sale, W. S. (2000). The 9 + 2 axoneme anchors multiple inner arm dyneins and a network of kinases and phosphatases that control motility. *J. Cell Biol.* **151**, F37-F§42.

Quarmby, L. M. (1996). Calcium influx activated by low pH in *Chlamydomonas. J. Gen. Physiol.* **108**, 351-361.

Rosenbaum, J. L. and Witman, G. B. (2002). Intraflagellar transport. *Nat. Rev. Mol. Cell. Biol.* **3**, 813-825.

Rosenbaum, J. L., Moulder, J. E. and Ringo, D. L. (1969). Flagellar elongation and shortening in *Chlamydomonas*. The use of cycloheximide and colchicine to study the synthesis and assembly of flagellar proteins. *J. Cell Biol.* **41**, 600-619.

Salisbury, J. L., Baron, A. T. and Sanders, M. A. (1988). The centrin-based cytoskeleton of *Chlamydomonas reinhardtii*: distribution in interphase and mitotic cells. *J. Cell Biol.* **107**, 635-641.

Sanders, M. A. and Salisbury, J. L. (1989). Centrin-mediated microtubule severing during flagellar excision in *Chlamydomonas reinhardtii*. *J. Cell Biol.* **108**, 1751-1760.

Tam, L. W., Dentler, W. L. and Lefebvre, P. A. (2003). Defective flagellar assembly and length regulation in LF3 null mutants in *Chlamydomonas*. *J. Cell Biol.* **163**, 597-607.

Umen, J. G. and Goodenough, U. W. (2001). Control of cell division by a retinoblastoma protein homolog in *Chlamydomonas*. *Genes Dev.* **15**, 1652-1661.

Umen, J. G., Le, H. and Fang, S. (2003). Cell-size control by the RB pathway in *Chlamydomonas*. *Mol. Biol. Cell* **14**, 10a.

Upadhya, P., Birkenmeier, E. H., Birkenmeier, C. S. and Barker, J. E. (2000). Mutations in a NIMA-related kinase gene, Nek1, cause pleiotropic effects including a progressive polycystic kidney disease in mice. *Proc. Natl. Acad. Sci. USA* **97**, 217-221.

Virca, G. D., Northemann, W., Sheils, B. R., Widera, G. and Broome, S. (1990). Simplified northern blot hybridization using 5% sodium dodecyl sulfate. *Biotechniques* **8**, 370-371.

Walther, Z., Vashishtha, M., Vashishtha, M. and Hall, J. L. (1994). The *Chlamydomonas* FLA10 gene encodes a novel kinesinhomologous protein. *J. Cell Biol.* **126**, 175-188.

Wilson, N. F. and Lefebvre, P. A. (2004). Regulation of flagellar assembly by glycogen synthase kinase 3 in *Chlamydomonas reinhardtii*. *Eukaryot. Cell* **3**, 1307-1319.

Witman, G. B. (1986). Isolation of *Chlamydomonas* flagella and flagellar axonemes. *Methods Enzymol.* **134**, 280-290.

Wloga, D., Rogowski, K. and Gaertig, J. (2003). NIMA-related kinases affect tubulin modifications and length of cilia in *Tetrahymena*. *Mol. Biol. Cell* **14**, 435a-436a.